Am J Physiol Endocrinol Metab 293: E1636–E1644, 2007.
First published September 11, 2007; doi:10.1152/ajpendo.00396.2007.

Distinct roles for intrinsic osteocyte abnormalities and systemic factors in regulation of FGF23 and bone mineralization in *Hyp* mice

Shiguang Liu, Wen Tang, Jianping Zhou, Luke Vierthaler, and L. Darryl Quarles

The Kidney Institute, University of Kansas Medical Center, Kansas City, Kansas

Submitted 22 June 2007; accepted in final form 7 September 2007

Liu S, Tang W, Zhou J, Vierthaler L, Quarles LD. Distinct roles for intrinsic osteocyte abnormalities and systemic factors in regulation of FGF23 and bone mineralization in *Hyp* mice. *Am J Physiol Endocrinol Metab* 293: E1636–E1644, 2007. First published September 11, 2007; doi:10.1152/ajpendo.00396.2007.—X-linked hypophosphatemia (XLH) is characterized by hypophosphatemia and impaired mineralization caused by mutations of the PHEX endopeptidase (phosphate-regulating gene with homologies to endopeptidases on the X chromosome), which leads to the overproduction of the phosphaturic fibroblast growth factor 23 (FGF23) in osteocytes. The mechanism whereby PHEX mutations increase FGF23 expression and impair mineralization is uncertain. Either an intrinsic osteocyte abnormality or unidentified PHEX substrates could stimulate FGF23 in XLH. Similarly, impaired mineralization in XLH could result solely from hypophosphatemia or from a concomitant PHEX-dependent intrinsic osteocyte abnormality. To distinguish between these possibilities, we assessed FGF23 expression and mineralization after reciprocal bone cross-transplantations between wild-type (WT) mice and the *Hyp* mouse model of XLH. We found that increased FGF23 expression in *Hyp* bone results from a local effect of PHEX deficiency, since FGF23 was increased in *Hyp* osteocytes before and after explantation into WT mice but was not increased in WT osteocytes after explantation into *Hyp* mice. WT bone explanted into *Hyp* mice developed rickets and osteomalacia, but *Hyp* bone explanted into WT mice displayed persistent osteomalacia and abnormalities in the primary spongiosa, indicating that both phosphate and PHEX independently regulate extracellular matrix mineralization. Unexpectedly, we observed a paradoxical suppression of FGF23 in juvenile *Hyp* bone explanted into adult *Hyp* mice, indicating the presence of an age-dependent systemic inhibitor of FGF23. Thus PHEX functions in bone to coordinate bone mineralization and systemic phosphate homeostasis by directly regulating the mineralization process and producing FGF23. In addition, systemic counter-regulatory factors that attenuate the upregulation of FGF23 expression in *Hyp* mouse osteocytes are present in older mice.

PHEX endopeptidase; X-linked hypophosphatemia; fibroblast growth factor 23; rickets; osteomalacia

X-LINKED HYPOPHOSPHATEMIA (XLH) is caused by inactivating mutations of the endopeptidase PHEX (phosphate-regulating gene with homologies to endopeptidases on the X chromosome) (32), a member of the M13 family of the type II cell-surface zinc-dependent proteases that is predominately expressed in bone (33). The mouse *Phex* cDNA sequence is highly homologous to that of humans, and a 3′ deletion of the *Phex* gene in the *Hyp* mouse results in an animal model of XLH (4, 29). PHEX mutations result in impaired renal tubular reabsorption of phosphate and aberrant regulation of $1,25(OH)_2D$ production, leading to hypophosphatemia and defective calcification of cartilage and bone, which result in rickets, osteomalacia, and growth retardation (32). Recent studies have indicated that the phosphaturia and impaired production of $1,25(OH)_2D$ in XLH are due to increased production of fibroblast growth factor 23 (FGF23) by osteocytes in bone (15). The causative role of FGF23 in *Hyp* mice is supported by the findings that crossing FGF23-null mice onto the *Hyp* background reverses the hypophosphatemia (28) and that blocking antibodies to FGF23 ameliorates hypophosphatemia and rickets in *Hyp* mice (1). In addition, FGF23 is the key phosphaturic factor underlying hereditary hypophosphatemic disorders, including autosomal-dominant hypophosphatemic rickets (ADHR), autosomal-recessive hypophosphatemic rickets, and XLH. Mutations in FGF23 that prevent its cleavage by furin-like proprotein convertases and mutations in DMP1 that stimulate FGF23 gene transcription cause ADHR and autosomal-recessive hypophosphatemic rickets, respectively (8, 16, 27, 31, 36).

FGF23 is a member of the fibroblastic growth factor family and is a critical hormonal regulator of systemic phosphate homeostasis. Circulating FGF23 targets Klotho-FGFR complexes in the kidney to inhibit sodium-dependent phosphate reabsorption and 1α-hydroxylase in the proximal tubule (10, 34). FGF23's phosphaturic activity and its ability to suppress $1,25(OH)_2D$ have been shown by administration of recombinant FGF23 to wild-type (WT) mice and overexpression of FGF23 in transgenic mice. Conversely, FGF23 deficiency (2, 3, 12, 24–26, 31, 37) or mutations increasing FGF23 degradation (11) result in hyperphosphatemia, increased serum $1,25(OH)_2D_3$ levels, and soft tissue calcifications.

The exact mechanism whereby mutations of PHEX cause elevated FGF23 is not known. Despite earlier reports to the contrary (6), FGF23 does not appear to be a PHEX substrate (5, 13). Rather, increased serum FGF23 levels correspond to increased production of FGF23 by osteocytes in the *Hyp* mouse model of XLH (13), indicating that PHEX mutations somehow stimulate FGF23 gene transcription. This might result from a PHEX-dependent intrinsic abnormality in osteocytes or from aberrant production of a humoral factor due to altered metabolism of unknown PHEX substrates. These possibilities have been inadequately explored, and previous studies have produced conflicting data. With regard to systemic factors, PHEX could either proteolytically inactivate an FGF23 stimulatory factor or activate a FGF23 suppressive factor that would respectively accumulate or be deficient in the presence of inactivating PHEX mutations. Although no physiologically relevant substrates for PHEX have been identified to date, the

Address for reprint requests and other correspondence: L. Darryl Quarles, 3901 Rainbow Blvd., MS 3018, Kansas City, KS 66160 (e-mail: dquarles@kumc.edu); or S. Liu, 3901 Rainbow Blvd., MS 3018, Kansas City, KS 66160 (e-mail: sliu@kumc.edu).

The costs of publication of this article were defrayed in part by the payment of page charges. The article must therefore be hereby marked "*advertisement*" in accordance with 18 U.S.C. Section 1734 solely to indicate this fact.

highly variable serum FGF23 levels in both patients with XLH (39) and ADHR (9) implicate additional factors that regulate circulating FGF23 concentrations beyond the causative mutations in these hereditary disorders. On the other hand, factors intrinsic to inactivating PHEX mutations in the local osteocyte microenvironment might regulate FGF23 gene transcription. In this regard, although PHEX is expressed in cells within the osteoblast lineage, including osteoblasts and osteocytes, FGF23 is selectively upregulated in osteocytes embedded in bone, but not in surface-lining osteoblasts derived from *Hyp* mice. The fact that PHEX is necessary but not sufficient to upregulate FGF23 expression is consistent with the requirement for additional factors related to terminal differentiation into osteocytes and/or matrix-derived factors to upregulate FGF23 in the setting of PHEX deficiency (15).

The mechanisms whereby inactivating PHEX mutations lead to defective mineralization of bone and cartilage is also not clear. Evidence that FGF23 directly targets bone cells is presently lacking (34). Rather, the bone mineralization defect in XLH appears to be due either to hypophosphatemia and/or to a nascent defect in osteoblast function that impairs the mineralization process. Several initial observations provide compelling support for an intrinsic defect in mineralization of extracellular matrix in PHEX-deficient osteoblasts (7, 18, 21, 38), possibly due to the production of a putative mineralization inhibitory factor called minhibin (38). More recently, however, the nascent defect in osteoblast-mediated mineralization in PHEX deficiency was brought into question, based on the observation that correction of hypophosphatemia alone significantly improved rickets and osteomalacia in *Hyp* mice (20). In addition, PHEX is expressed in chondrocytes, and loss of PHEX in *Hyp* mice leads to a widened hypertrophic zone and impaired mineralization, retained cartilage remnants, and abnormal resorption of the subchondral primary spongiosa. These effects could also be due to hypophosphatemia or intrinsic abnormalities in PHEX-deficient chondrocytes (19).

Thus, although elevated FGF23 is a fundamental abnormality in XLH rickets, it remains unknown whether the increased production of FGF23 by osteocytes is the consequence of an intrinsic bone abnormality or aberrant production of another upstream factor resulting from inactivating PHEX mutations. In addition, it remains unclear to what extent the mineralization defect of bone and cartilage in XLH is due to local actions of PHEX or to systemic changes in phosphate and vitamin D metabolism induced by FGF23. In the present study, we developed a technique for bone explantation to comprehensively examine whether FGF23 regulation and bone mineralization result from an intrinsic or systemic effects of PHEX mutations. Assessment of FGF23 expression and bone mineralization in bone from WT mice engrafted into *Hyp* mice with an altered hormonal/metabolic milieu and in bone from mutant *Hyp* mice transplanted into a WT mouse with a normal hormonal/metabolic milieu permit examination of the relative importance of intrinsic and systemic effects of inactivating PHEX mutations.

MATERIALS AND METHODS

Animals and genotyping. The FGF23-eGFP reporter mouse model was created by knocking in an enhanced green fluorescent protein (eGFP) reporter by replacing exon 1 of the *Fgf23* gene with eGFP cDNA as described previously (15). The FGF23-eGFP reporter mice used in the embryo experiment and the bone explantation experiment in the present study were in a 129Sv/Ev and C57BL/6J mixed genetic background and a C57BL/6J genetic background, respectively. The mice were genotyped with the REDExtract-N-Amp tissue PCR kit (Sigma-Aldrich, St. Louis, MO) with the following primers: for FGF23, 5′-CTGACCTCTGATGGCACTGA-3′ (forward) and 5′-GAAGATTGTTCGCACAGCAA-3′ (reverse); for Neo, 5′-ATTCG-GCAAGCAGGCATC-3′ (forward) and 5′-CTGTTCTCCTCTTCCT-CATCTC-3′ (reverse) for FGF23-null mice; and for PHEX19, 5′-GCTTGGGCTAGTTTGCTATCT-3′ (forward) and 5′-TGAGTTGGTGC-TATACACGGAG-3′ (reverse) for *Hyp* mice.

All mice were fed the Labdiet JL rat and mouse/auto 6F diet (Labdiet, Brentwood, MO) containing 1.15% calcium and 0.85% phosphorus and tap water. All mice were maintained and used in accordance with recommendations in the *Guide for the Care and Use of Laboratory Animals* (Institute for Laboratory Animal Research, National Research Council, Washington, DC: National Academy Press, 1996), and experiments were reviewed and approved by the Institutional Animal Care and Use Committee (protocol number 2007-1632).

Intramuscular bone explantation. Intramuscular bone explantations were modified by using a previously reported method (30). To generate WT and *Hyp* newborn mice carrying the FGF23-eGFP reporter, male WT/FGF23-eGFP$^{+/-}$ and female *Hyp*/FGF23-eGFP$^{+/-}$ mice were mated. Newborn male mice at 4.5 days old were genotyped by PCR. Then, male WT and *Hyp* newborn mice carrying FGF23-eGFP reporter (WT/FGF23-eGFP$^{+/-}$ and *Hyp*/FGF23-eGFP$^{+/-}$, respectively) were euthanized, and both tibias and femurs were isolated and explanted into the back muscles of 8- to 10-wk-old WT and *Hyp* male mice. The tibias or femurs from one side were explanted to WT mice, and the tibias or femurs from the other side were explanted to *Hyp* mice. Each host mouse received one explanted bone on each side of its back muscles. Three weeks after explantation, explanted bones were harvested to measure bone length and were examined by X-ray radiography, microcomputer tomography, and histological analysis. Serum samples from the host mice were also collected for serum biochemical assays.

In some studies, long bones from *Hyp* mice were first transplanted into WT and *Hyp* mice for a 3-wk period and then reexplanted into *Hyp* and WT mice, respectively, for an extra 2-wk period. The explanted bones were then harvested for histological eGFP assessment. To see the fluorescent labeling in bone, some mice explanted with femurs were prelabeled by intraperitoneal injection with alizarin complex one (10 mg/kg; Acros Organics, Fair Lawn, NJ) and calcein (5 mg/kg; Sigma-Aldrich) 4 and 1 days, respectively, before the mice were killed.

Embryo studies. To examine whether a circulating factor exists in *Hyp* mice to stimulate FGF23 promoter, we mated male WT/FGF23-eGFP$^{+/-}$ with female *Hyp* mice to obtain pregnant *Hyp* mice bearing both WT/FGF23-eGFP$^{+/-}$ and *Hyp*/FGF23-eGFP$^{+/-}$ embryos. We also mated male *Hyp*/FGF23-eGFP$^{+/-}$ with WT female mice to obtain pregnant WT mice bearing both WT/FGF23-eGFP$^{+/-}$ and *Hyp*/FGF23-eGFP$^{+/-}$ embryos. We isolated both *Hyp* and WT embryos carrying the FGF23-eGFP reporter gene at embryonic *day 17.5* from both pregnant *Hyp* and pregnant WT mice. The femurs were dissected from the embryos and fixed in 4% paraformaldehyde for cryosection. The eGFP expression in osteocytes was compared among WT embryos in WT mothers, WT embryos in *Hyp* mothers, *Hyp* embryo in WT mothers, and *Hyp* embryos in *Hyp* mothers.

Histological analysis. eGFP fluorescent imaging in bone was performed with previously described methods (15). Briefly, mouse bones were quickly dissected and fixed in 4% paraformaldehyde in PBS (pH 7.4) and then embedded in frozen embedding medium. Cryosectioning was performed on a Leica CM1900 cryostat (D-69226; Leica, Nussloch, Germany) equipped with a CryoJane frozen sectioning kit

(Instrumedics, Hackensack, NJ). Sections (5 μm) were obtained from embedded bone samples. eGFP was examined with a Leica DM IRB inverted microscope equipped with a Leica DM 500 digital camera. The frozen sections were also stained with Von Kossa's stain and analyzed under bright-field microscopy.

Explanted femurs prelabeled with alizarin complex one and calcein were collected and fixed in 70% ethanol and embedded in methyl methacrylate. Sections (5 μm) were stained with Goldner's stain and analyzed under microscope with transmitted light. Unstained sections (10 μm) were evaluated under UV light. Quantitative analysis of bone sections was performed with the OsteoMeasure bone histomorphometry system (OsteoMetrics, Atlanta, GA). The following static and dynamic parameters were measured: osteoid volume (%), osteoid surface (%), osteoid seam thickness (μm), mineralizing osteoid (%), bone formation rate ($\mu m^3 \cdot \mu m^{-2} \cdot day^{-1}$), bone formation rate/bone surface referant, and mineralization lag time (day) (22).

High-resolution radiography, bone densitometry, and microcomputed tomography analysis of femurs. Bone samples were fixed in 70% ethanol after they were harvested from the animals. The radiography of femurs was performed with the Faxitron specimen radiography system MX-20 (Faxitron X-Ray, Wheeling, IL). Bone mineral density (BMD) of femurs was measured with the use of a PIXImus bone densitometer (Lunar, Madison, WI). High-resolution microcomputed tomography (μCT40; Scanco Medical, Basserdorf, Switzerland) was used to scan and evaluate bone volume fraction and BMD in the femurs as previously described (15). Briefly, bone samples were scanned in a sample holder with 10.2 mm diameter at medium resolution. The three-dimensional images were generated with the built-in software using a threshold of 250. The mineralized tissue volume fractions were evaluated from the beginning of calcified tissue underneath the growth plate to the midpoint of the distal femur to adjust for the different bone lengths. The region of interest for quantitative analysis was manually drawn.

Serum biochemical measurements. Serum biochemical measurements were performed as previously described (15). Briefly, serum FGF23 levels were measured using an FGF23 ELISA kit (Kainos Laboratories, Tokyo, Japan), serum calcium was measured using a colorimetric assay (Stanbio Laboratories, Boerne, TX), and serum phosphorus was measured by the phosphomolybdate-ascorbic acid method.

Statistics. We evaluated differences between the WT and *Hyp* preexplantation and postexplantation by both two-way and factorial ANOVA. A Tukey's post hoc test was subsequently performed with the adjusted *P* values. For multiple group comparison in quantitative histomorphometric analysis of postexplanted bone sections, one-way ANOVA and Tukey's post hoc test were used to determine differences among groups. Results were considered to be significantly different at $P < 0.05$. All values are expressed as means ± SE. Computations were performed using either GraphPad Prism (GraphPad Software, San Diego, CA) or STATISTICA (StatSoft, Tulsa, OK).

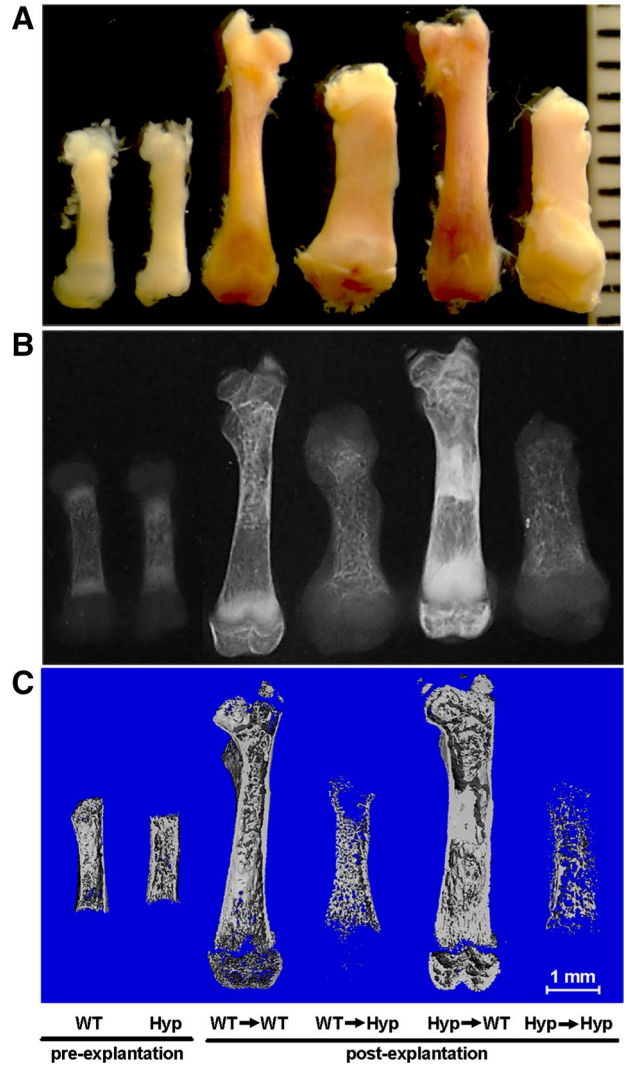

Fig. 1. Gross appearance and radiological analysis of femurs from wild-type (WT) and *Hyp* mice before and after explantation. Shown are gross appearance images (*A*), radiographs (*B*), and 3-dimensional microcomputed tomography images (*C*) of femurs obtained from WT/FGF23$^{+/-}$ and *Hyp*/FGF23$^{+/-}$ mice (where FGF23 is fibroblast growth factor 23) before explantation and 3 wk after explantation into WT and *Hyp* adult mice as indicated. Femurs of 4.5-day-old WT/FGF23$^{+/-}$ and *Hyp*/FGF23$^{+/-}$ reporter mice were explanted into the back muscles of WT and *Hyp* adult mice as described in MATERIALS AND METHODS.

RESULTS

Effects of autologous bone explantation. Initially, we evaluated growth and mineralization characteristics of bone from 4.5-day-old WT and *Hyp* mice expressing eGFP under the control of the FGF23 promoter after explantation into mice of the same genetic background (e.g., WT into WT and *Hyp* into *Hyp*). The gross appearance and length of bones at the time of isolation were similar between WT and *Hyp* mice (Fig. 1*A*; Table 1), indicating that the full features of rickets and osteomalacia had not yet emerged. However, Faxitron radiography and microcomputed tomography identified increased bone volume in the metaphyseal region of *Hyp* mice (Fig. 1, *B* and *C*) that resulted in a measurable increase in BMD and in metaphyseal mineralized tissue volume (Table 1). Analysis of preexplant bone revealed the presence of normal bone architecture and bone histology in WT mice, as expected; however, rickets and osteomalacia were present in *Hyp* bone at 4.5 days of age. This was evidenced by the widened growth plate and excess unmineralized osteoid on bone surfaces (Fig. 2, *A* and *B*). Consistent with increased FGF23 production in osteocytes of *Hyp* mice, we observed eGFP expression in osteocytes of *Hyp* mice and no detectable eGFP in WT mice at 4.5 days of age (Fig. 3*A*).

We found that the bone explanted into muscles remained viable and increased in size over the 3-wk observation period (Fig. 1). Explantation of bone between donor and recipient of the same genotype produced bone morphogenic changes consistent with those observed during bone development in the intact animal. In this regard, WT bone explanted into WT

Table 1. *Bone length and radiological analysis of femurs from WT and Hyp mice before and after explantation*

Variable	Preexplantation		Postexplantation				ANOVA Effects (*P* value)		
	WT	*Hyp*	WT in WT	WT in *Hyp*	*Hyp* in WT	*Hyp* in *Hyp*	Genotype	Explantation	Host Genotype
Femur length, mm	5.2±0.1	5.5±0.1*	8.8±0.1	6.8±0.2†	8.9±0.2	7.0±0.1†‡	0.0012	<0.0001	<0.0001
BMD, g/cm^2	0.014±0.001	0.016±0.001*	0.019±0.006	0.008±0.002†	0.028±0.001*	0.0075±0.002†‡	<0.0001	NS (0.59)	<0.0001
Mineralized tissue volume, %	14.0±1.3	26.8±2.9*	19.1±1.1	7.6±1.5†	43.0±1.8*	5.2±1.0†‡	<0.0001	NS (0.67)	<0.0001

Values are means ± SE from at less 6 samples from each group. BMD, bone mineral density; NS, not significant. Statistical difference is defined when *P* value is <0.05. *Significantly different between wild-type (WT) and *Hyp* bones before explantation and WT and *Hyp* bone explanted into hosts with the same genotype. †Significantly different between WT or *Hyp* bone hosts in mice with different genotype. ‡Significantly different from WT in WT.

recipients after 3 wk had a normal gross appearance (Fig. 1*A*), had increased in length from 5.5 ± 0.1 to 8.8 ± 0.1 mm ($P < 0.001$, $n \geq 6$ in each group) (Table 1), and had no identifiable abnormalities detectable by radiography and microcomputed tomography (Fig. 1*B* and *C*). WT bone explanted into WT mice also retained a normal histological appearance of the growth plate and bone. Trabecular and cortical bone were characterized by narrow osteoid seams (Fig. 2*B*) and distinct fluorescent labels consistent with ongoing mineralization (Fig. 2*C*). No eGFP expression, a marker of FGF23 promoter activity, was detected in osteocytes from WT mice after explantation (Fig. 3*B*).

In contrast, *Hyp* bone explanted into *Hyp* mice displayed growth retardation and evidence of rickets and osteomalacia, as detected by radiography and microcomputed tomography (Fig. 1). The change in length of the *Hyp* femurs explanted into *Hyp* was small (from 5.2 ± 0.10 to 7.0 ± 0.12 mm; $P > 0.05$, $n \geq 6$). Moreover, we observed evidence of widened growth plates and decreased BMD and mineralized tissue volume in explanted *Hyp* bone compared with WT bone explanted into WT mice (Fig. 1 and Table 1). Histological examination confirmed

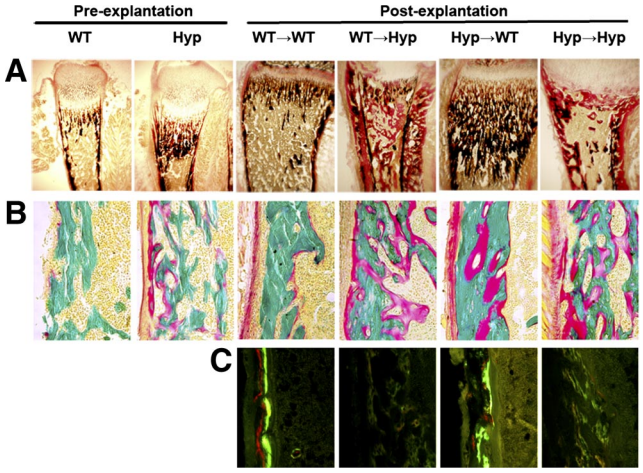

Fig. 2. Effects of bone cross-explantation on bone histology. *A*: von Kossa-stained sections from tibias of WT/FGF23$^{+/-}$ and *Hyp*/FGF23$^{+/-}$ mice at 4.5 days of age before and after explantation viewed under transmitted light (×25). Mineralized tissue stains black, and unmineralized osteoid stains red. *B*: Goldner-stained sections from distal femurs before and after explantation. Mineralized bone stains blue-green, and unmineralized osteoid stains orange-red. Shown are endochondral bone and adjacent trabecular structures from femurs obtained from the indicated genotypes before and after explantation (×200). *C*: micrographs viewed under fluorescent light showing alizarin red and calcein fluorescent labels in unstained sections of femurs after explantation (×200).

the widened growth plate and excess osteoid (Fig. 2, *A* and *B*). In addition, diffuse fluorescent labels were present in explanted *Hyp* bone, consistent with defective mineralization (Fig. 2*C*). Surprisingly, the increase in eGFP expression in osteocytes of *Hyp* mice preexplantation (Fig. 3*A*, *right*) was lost in *Hyp* bone explanted into *Hyp* mice (Fig. 3*B*), suggesting the presence of a circulating FGF23 suppressive factor (see below).

Effects of cross-explantation of bone between WT and Hyp mice. Next, we examined the effects of bone cross-explantation in WT and *Hyp* mice with donors and recipients of different genotypes. Three weeks after surgery, WT femurs explanted into *Hyp* mice demonstrated slower growth rates (from 5.5 ± 0.1 to 6.8 ± 0.2 mm; $P < 0.001$, $n \geq 6$ in each group) and exhibited gross features of *Hyp* bone (Fig. 1 and Table 1). In this regard, WT bone explanted into *Hyp* mice acquired a widened metaphysisis, consistent with rickets (Fig. 1) and developed decreased BMD and mineralized tissue volume (Table 1). Histologically, WT bone in the *Hyp* mouse developed excess osteoid due to increased extent and width of osteoid seams and exhibited impaired mineralization, as evidenced by diffuse fluorescent labels and the complete absence of double labels (Fig. 1 and Table 2). Quantitative histological analysis of WT bone explanted into *Hyp* mice confirmed that exposure to the *Hyp* milieu resulted in increased relative osteoid volume, osteoid surface, and osteoid thickness compared with WT bone explanted into WT mice (Table 2). WT bone explanted into *Hyp*, however, failed to upregulate eGFP expression (Fig. 3*B*), suggesting that stimulation of FGF23 in *Hyp* is not due to a systemic factor but represents an intrinsic osteocyte defect.

In contrast, *Hyp* bone explanted into WT mice largely rescued the ricketic appearance of bone (Fig. 1). However, additional abnormalities were present, consisting of osteosclerotic-like changes in subchondral bone (Fig. 1), leading to increases in BMD and mineralized tissue volume to values greater than WT bone explanted into WT mice (Table 1). By bone histological evaluation, we found, after explantation of *Hyp* bone into the WT milieu, near normalization of the growth plate width, although there was persistence of previously described *Hyp*-related changes in the subchondral bone (19). These subchondral abnormalities included a widened zone of primary spongiosa, which contained cartilage remnants and abnormal resorption of mineralized tissue in the metaphyseal region (Fig. 4), which explain the sclerotic-looking changes observed by radiography and microcomputed tomography (Fig. 1 and Table 1). In addition, examination of bone also revealed excessive amounts of unmineralized osteoid and nar-

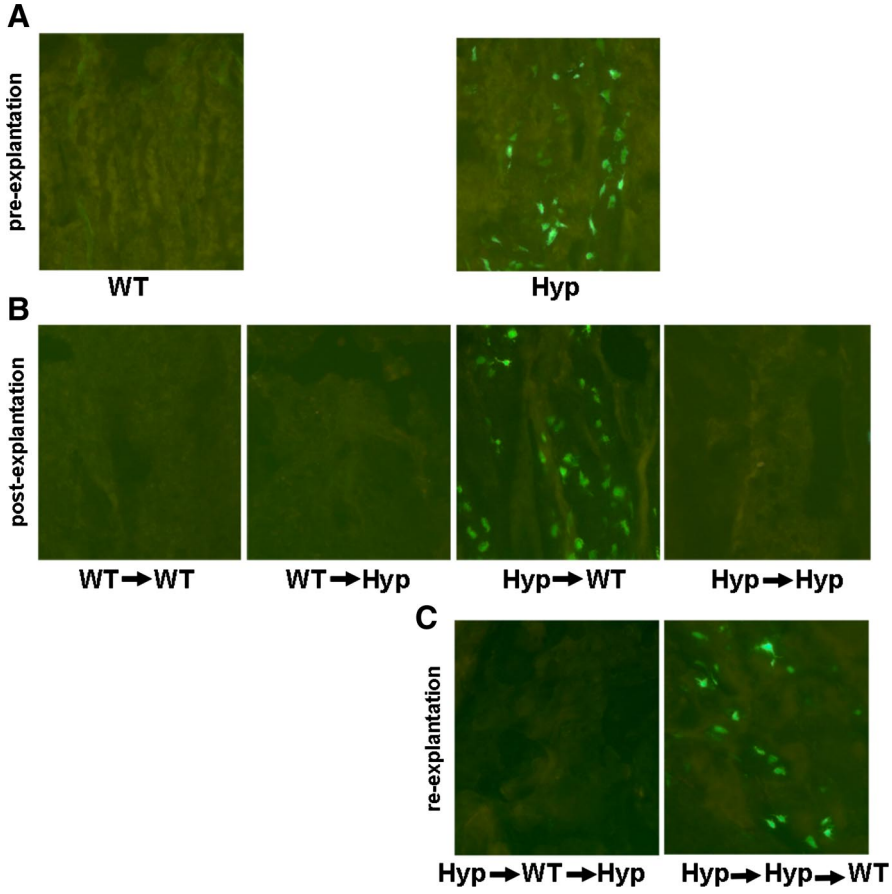

Fig. 3. FGF23 expression before and after bone explantation. *A*: increased expression of FGF23 in osteocytes of *Hyp* mice. Images are of frozen sections of femurs obtained from WT/FGF23$^{+/-}$ and *Hyp*/FGF23$^{+/-}$ neonates at 4.5 days of age viewed under fluorescent light. FGF23 promoter activity is measured by enhanced green fluorescent protein (eGFP) expression and is present in osteocytes of *Hyp* mice, consistent with increased FGF23 production in association with inactivating PHEX (phosphate-regulating gene with homologies to endopeptidases on the X chromosome) mutations. *B*: effect of cross-explantation on FGF23 expression. Images of frozen sections were obtained from WT bone explanted into either WT or *Hyp* mice (WT→WT and WT→*Hyp*) or *Hyp* bone explanted in WT or *Hyp* (*Hyp*→WT and *Hyp*→*Hyp*) (×200). *C*: reverse reexplantation of explanted bone. *Hyp* bone explanted into *Hyp* or WT mice was removed and reimplanted into WT or *Hyp* mice as described in MATERIALS AND METHODS. Return of *Hyp* bone to the WT milieu restored FGF23 expression in osteocytes. The micrographs represent frozen sections viewed under fluorescent light (×200).

row distances between the fluorescent labels, consistent with persistent impairment of mineralization (Fig. 2, *B* and *C*). The presence of osteomalacia was confirmed by quantitative histological analysis of the explanted bone, which showed increased relative osteoid volume, osteoid surface, and osteoid thickness and increased mineralization lag time (Table 2). Except for a measurable bone formation rate due to the presence of a few discernable double-labeled surfaces, the degree of osteomalacia in *Hyp* bone explanted into WT was similar to that of WT bone explanted into *Hyp* mice (Table 2). Because explantation of *Hyp* bone into WT mice did not alter serum phosphate (data not shown), these findings suggest that PHEX deficiency per se may be regulating bone mineralization. Moreover, FGF23 expression as assessed by eGFP remained elevated in *Hyp* bone transplanted into WT mice, consistent with PHEX mutations, leading to an intrinsic osteocyte defect in *Hyp* (Fig. 3*B*).

Further evidence for an intrinsic defect in Hyp leading to elevated FGF23 expression. To further confirm that the elevated FGF23 expression in osteocytes in *Hyp* mice is not caused by a circulating stimulatory factor in *Hyp* mice, we compared FGF23 promoter activities in osteocytes in femurs from WT/FGF23$^{+/-}$ and *Hyp*/FGF23$^{+/-}$ embryos at *day 17.5* from pregnant WT and *Hyp* mothers, respectively (Fig. 5). We found that eGFP expression was increased in osteocytes from PHEX-deficient *day 17.5 Hyp* embryos but not in osteocytes of WT littermates, regardless of the maternal genotype, indicating that increased FGF23 production by osteocytes is a nascent defect rather than being due to circulating maternal-derived factors.

Additional evidence for induction of an FGF23 suppressive factor with age in Hyp mice. To further explore whether the paradoxical suppression of FGF23 expression in *Hyp* bone transplanted into *Hyp* mice represents the presence of additional factors capable of suppressing FGF23 production, we removed the *Hyp* bone explanted into *Hyp* mice and reimplanted it into WT mice, as well as took *Hyp* bone explanted into WT mice that continued to express eGFP and reimplanted it into *Hyp* mice. Two weeks after reimplantation in WT mice, we found that the *Hyp* bone, which had lost eGFP expression in *Hyp* mice, regained eGFP expression after being reexplanted in WT mice. On the other hand, *Hyp* bone that initially retained eGFP expression in WT mice lost eGFP expression after being reexplanted in *Hyp* mice (Fig. 3*C*).

Because donor bone from *Hyp* mice is younger than that from recipient mice, we explored whether age-dependent suppression of FGF23 occurs in *Hyp* mice. For these studies, we compared eGFP expression as a measure of FGF23 promoter activity and circulating FGF23 levels in *Hyp* mice at ages ranging from 10 days to 12 wk (Fig. 6). We found that both FGF23 promoter activity in osteocytes in *Hyp* bones (Fig. 6*A*) and serum FGF23 levels (Fig. 6*B*) are highly elevated in *Hyp* mice up to 3 wk of age. Thereafter, both osteocyte expression and serum levels decline by 6 and 12 wk of age, indicating an age-dependent suppression in FGF23.

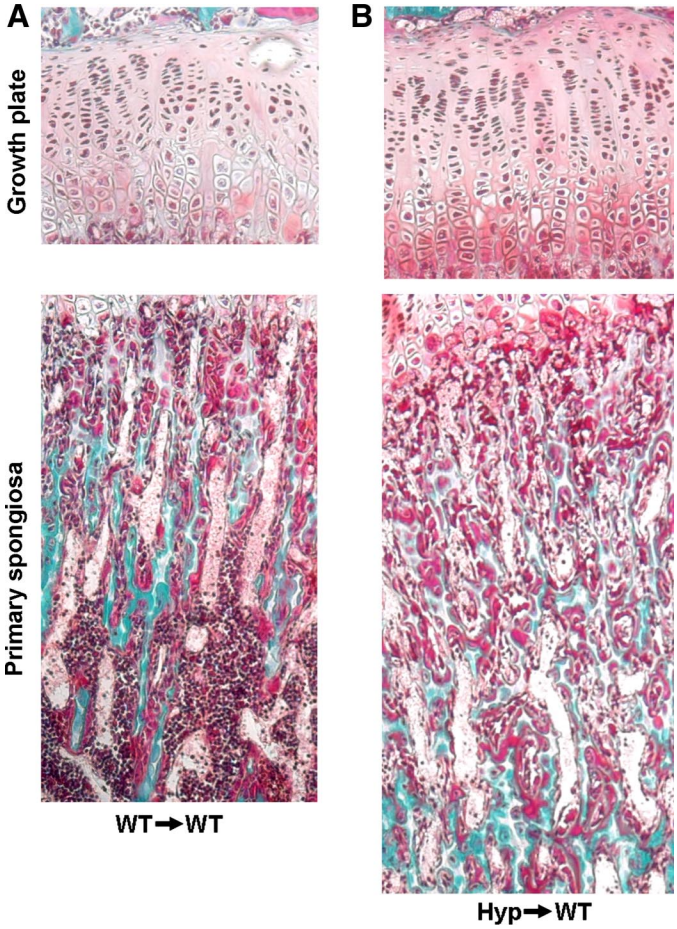

Fig. 4. Effects of bone explantation on growth plate cartilage and primary spongiosa. *A*: growth plate of WT bone explanted into a WT mouse showing normal resting, proliferating, and hypertrophic zones of cartilage (*top*) and remodeling of the subchondral region (*bottom*) as evidenced by vascular channels, calcified cartilage, and areas of resorption. *B*: growth plate of *Hyp* bone explanted into a WT mouse showing near normalization of the growth plate architecture (*top*) but expansion of the primary spongiosa due to retained cartilage elements and abnormal subchondral remodeling (*bottom*). Micrographs represent Goldner-stained sections (×200).

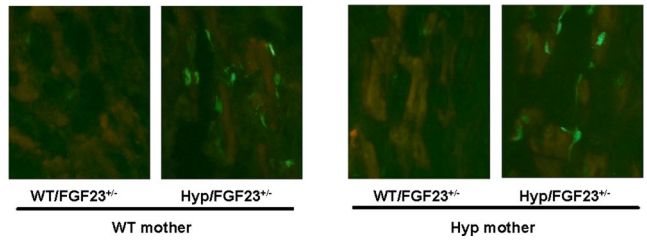

Fig. 5. Analysis of FGF23 promoter activities in osteocytes of femurs from *day 17.5* WT/FGF23$^{+/-}$ and *Hyp*/FGF23$^{+/-}$ embryos derived from either WT or *Hyp* pregnant mothers. From *left* to *right* shows, respectively, frozen sections of femurs from WT/FGF23$^{+/-}$ and *Hyp*/FGF23$^{+/-}$ embryos of pregnant WT female mice and WT/FGF23$^{+/-}$ and *Hyp*/FGF23$^{+/-}$ embryos of pregnant *Hyp* female mice viewed under fluorescent light (×200).

DISCUSSION

PHEX is a cell surface endopeptidase expressed predominantly in bone. Inactivating PHEX mutations lead to inhibition of renal phosphate reabsorption and 1,25$(OH)_2$D production in the kidney proximal tubule by increasing the production of FGF23 by osteocytes. How PHEX regulates FGF23 levels has not been established, and previous studies suggesting possible mechanisms have produced conflicting results. For example, after an initial study on purported PHEX-dependent cleavage of FGF23, subsequent studies found that FGF23 is not a substrate for PHEX (5, 13). Additional studies found that the production of FGF23 by osteocytes was increased in the setting of PHEX mutations (15). These findings suggested an alternative hypothesis that PHEX mutations may indirectly stimulate FGF23 production in osteocytes through the accumulation of yet to be identified extracellular PHEX substrates (14, 15). In the present study, we used bone cross-explantation between WT and *Hyp* mice to comprehensively examine the influence of local and systemic regulation of FGF23 by osteocytes in vivo. This experimental approach allowed us to examine the function of bone from *Hyp* mice in a normal hormonal/metabolic milieu and the function of normal bone in the abnormal metabolic environment of the *Hyp* mouse, thereby permitting additional insights into how PHEX mutations regulate FGF23 expression. We found that the bone explantation procedure does not alter growth or mineralization of the explanted bone. Indeed, both bone and growth plate development progressed normally in bone explanted into WT mice. The surgical procedure, therefore, did not confound interpretation of data from the cross-explantation studies.

In contrast to the possibility that accumulation of PHEX substrates stimulates FGF23 production, our observations support the alternative hypothesis that FGF23 production by osteocytes is an intrinsic defect derived from inactivating PHEX mutations in these cells. In this regard, inactivating mutations of PHEX in *Hyp* mice result in the increased production of FGF23 in osteocytes, and this increase in FGF23 expression in *Hyp* bone is retained when transferred to the normal hormonal/metabolic milieu of the WT mouse. In contrast, cross-explantation of WT bone into *Hyp* did not result in increased FGF23

Table 2. *Histomorphometric analysis of explanted bones*

Index	WT in WT	WT in *Hyp*	*Hyp* in WT	*Hyp* in *Hyp*	*P* Value
OV/BV, %	7.7±1.1[a]	33.1±5.1[b,c]	27.7±3.2[b]	38.0±2.2[c]	0.0001
OS/BS, %	21.8±0.9[a]	48.2±5.3[b]	49.0±6.2[b]	50.8±7.4[b]	0.0080
OTh, μm	5.0±0.5[a]	13.2±1.3[b,c]	11.2±1.4[b]	16.5±1.7[c]	0.0004
MS/OS. %	89.4±21.1[c]	0.0[a]	16.2±0.7[b]	0.0[a]	0.0002
BFR/BS, $\mu m^3/\mu m^2$	0.42±0.12[c]	0.0[a]	0.10±0.01[b]	0.0[a]	0.0012
MLT, day	3.5±1.2[a]	∞	79.8±20.3[b]	∞	

Values are means ± SE. OV/BV, ratio of osteoid volume to bone volume; OS/BS, ratio of osteoid surface to bone surface; OTh, osteoid seam thickness; MS/OS, ratio of mineralizing osteoid to osteoid surface; BFR, bone formation ratio; MLT, mineralization lag time. ∞, Value could not be calculated because of no measurable double labels. Values sharing the same superscript within a category across genotypes are not significantly different by $P < 0.05$.

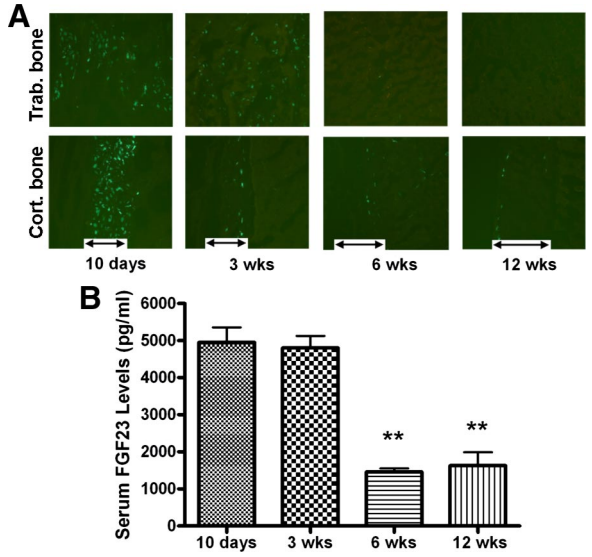

Fig. 6. Age-dependent FGF23 promoter activities in osteocytes and corresponding serum FGF23 levels in *Hyp* mice. *A*: FGF23 promoter activity is indicated by eGFP expression using fluorescent microscopy (×200) in osteocytes of trabecular (Trab; *top*) and cortical (Cort; *bottom*) bone as a function of age in *Hyp* mice. FGF23 promoter activity decreases by 6 wk of age. *B*: serum FGF23 levels in 10-day and 3-, 6- and 12-wk-old mice. Data are means ± SE from 4–6 mice in each group. **Values significantly different from 10-day old mice ($P < 0.01$).

expression in osteocytes, further indicating the absence of a humoral factor in *Hyp* capable of stimulating FGF23 production. The absence of a circulating FGF23 stimulatory factor was confirmed in studies of embryos in *Hyp* mothers, which also expressed FGF23 only in embryos with the inactivating PHEX mutation. Thus the increased expression of FGF23 in osteocytes, both in the cross-explantation and embryo models, corresponds to the bone genotype but not the hormonal/metabolic milieu. The proximate signal linking PHEX to FGF23 expression remains to be identified, but additional data suggest that factors in the bone extracellular matrix, such as dentin matrix protein 1, may participate in the upregulation of FGF23 (8, 15).

In contrast to this intrinsic regulation of FGF23, we also found evidence for a putative hormonal/metabolic change in older *Hyp* mice that suppresses FGF23 production, thereby attenuating the intrinsic defect leading to increased FGF23 in younger *Hyp* mice. In this regard, transplantation of *Hyp* bone into *Hyp* mice paradoxically resulted in loss of FGF23 expression in osteocytes. This loss of FGF23 is not due to gross abnormalities in bone development or osteocyte viability, since the bone grows in size and osteocytes are present. In addition, we confirmed that this was not due to the surgical intervention by reimplanting the explanted *Hyp* bone back into a WT mouse. The reimplanted *Hyp* bone regained its high level of FGF23 expression in osteocytes when returned to the WT environment. Conversely, reimplanting *Hyp* bone that had previously been cross-explanted into WT mice and that displayed high levels of FGF23 expression lost FGF23 expression when transferred to the *Hyp* mouse. To explore the potential for an age-dependent suppression of FGF23, since we implanted younger bone into older mice, we examined FGF23 expression in *Hyp* mice at different ages (Fig. 6). We found a concordant suppression of FGF23 circulating levels and bone expression in older mice. The loss of FGF23 production appears to be due to either the presence of an inhibitory factor or the loss or degradation of an FGF23 stimulatory factor. Moreover, other evidence does exist that supports the existence of yet to be identified humoral factors that regulate FGF23. For instance, recent studies of selective vitamin D receptor deletion in cartilage identified the production of putative factors by chondrocytes that regulate FGF23 expression in bone (17). In addition, clinical observations that FGF23 levels are highly variable in humans (such as in XLH and ADHR, which are known to be caused by FGF23) (9, 35) support the presence of factors that regulate FGF23 independent of PHEX. The existence of putative hormonal or metabolic inhibitors in older *Hyp* mice may also reflect an adaptive response of the *Hyp* mice to suppress the elevated FGF23 in the younger *Hyp* mice. Moreover, a suppressive factor for FGF23 may have important implications with regard to treatment of children with hypophosphatemic rickets and may explain why the disease appears to lessen in severity with age (23).

Impaired mineralization of bone is also observed in XLH or *Hyp* mice. Studies attempting to discern the possible direct role of PHEX from secondary effects of hypophosphatemia on extracellular matrix mineralization have also produced conflicting results. An intrinsic defect in osteoblasts or osteocytes caused by PHEX deficiency is supported by both in vivo and in vitro observations (7, 18, 38). In this regard, osteoblasts from *Hyp* mice, when transplanted into WT mice or grown in culture, produce abnormally mineralizing extracellular matrix, consistent with a functional effect of PHEX deficiency in bone-forming cells (7, 38). However, these data are difficult to reconcile with more recent studies showing that*Hyp* osteoblasts cultured in the presence of phosphate mineralize extracellular matrix to the same extent as WT osteoblasts and the finding that feeding *Hyp* mice a high-phosphorus diet results in almost complete rescue of the bone mineralization defect (20). These latter findings suggest that hypophosphatemia, rather than an intrinsic osteoblast defect, is primarily responsible for impaired mineralization of extracellular matrix (20).

Our study provides insights into the relative importance of hypophosphatemia and intrinsic osteoblast defect. On the one hand, the observations that WT bones explanted into *Hyp* mice for 3 wk developed defective mineralization, as evidenced by increased unmineralized osteoid and diffuse fluorescent labeling (Fig. 2), suggest that the impaired mineralization is largely a consequence of the hypophosphatemic *Hyp* milieu. On the other hand, *Hyp* bone explanted into WT mice also displayed impaired mineralization, as evidenced by the excess osteoid and impaired fluorescent labeling of bone. Moreover, the abnormalities of subchondral bone observed in juvenile *Hyp* mice before explantation and bone from *Hyp* mice explanted into the WT milieu reflect the previously reported abnormalities in primary spongiosa associated with PHEX mutations (19). Together, these findings suggest the presence of an intrinsic mineralization defect related to PHEX mutations in both osteoblasts and chondrocytes. An alternative possibility that FGF23 might also stimulate osteoblast-mediated matrix production is not supported by existing data, which indicate that osteoblasts are not targets for FGF23 actions (34).

In summary, the present findings provide unequivocal evidence that the mechanism whereby PHEX mutations lead to increased FGF23 expression in osteocytes is intrinsic to bone.

In addition, we observed for the first time the possible presence of putative circulating factors that mitigate the increase in FGF23 production in older *Hyp* mice. Our studies also support the presence of an intrinsic mineralization defect related to PHEX mutation in osteoblasts/osteocytes that is modified by the humoral/metabolic milieu. A complete understanding of the molecular pathogenesis of XLH will require future studies to define the exact mechanisms for the stimulation of osteocyte production of FGF23 by PHEX-dependent changes in the bone microenvironment, to identity the putative circulating factor that reduces FGF23 expression in the adult *Hyp* mouse, and to characterize the local factors responsible for PHEX-dependent regulation bone extracellular matrix mineralization.

ACKNOWLEDGMENTS

We thank Steffani Webb for editorial assistance and Dr. Valentin David for assistance on statistical analysis.

GRANTS

The project described was supported by National Institute of Arthritis and Musculoskeletal and Skin Diseases Grant RO1 AR-45955 and National Center for Research Resources Grant P20 RR-17708.

REFERENCES

1. **Aono Y, Shimada T, Uamazaki Y, Hino R, Takeuchi Y, Fujita T, Fukumoto S, Nagano N, Wada M, Yamashita T.** The neutralization of FGF-23 ameliorates hypophosphatemia and rickets in *Hyp* mice (Abstract). *J Bone Miner Res* 18: S16, 2003.
2. **Bai X, Miao D, Li J, Goltzman D, Karaplis AC.** Transgenic mice overexpressing human fibroblast growth factor 23 (R176Q) delineate a putative role for parathyroid hormone in renal phosphate wasting disorders. *Endocrinology* 145: 5269–5279, 2004.
3. **Bai XY, Miao D, Goltzman D, Karaplis AC.** The autosomal dominant hypophosphatemic rickets R176Q mutation in fibroblast growth factor 23 resists proteolytic cleavage and enhances in vivo biological potency. *J Biol Chem* 278: 9843–9849, 2003.
4. **Beck L, Soumounou Y, Martel J, Krishnamurthy G, Gauthier C, Goodyer CG, Tenenhouse HS.** Pex/PEX tissue distribution and evidence for a deletion in the 3′ region of the Pex gene in X-linked hypophosphatemic mice. *J Clin Invest* 99: 1200–1209, 1997.
5. **Benet-Pages A, Lorenz-Depiereux B, Zischka H, White KE, Econs MJ, Strom TM.** FGF23 is processed by proprotein convertases but not by PHEX. *Bone* 35: 455–462, 2004.
6. **Bowe AE, Finnegan R, Jan de Beur SM, Cho J, Levine MA, Kumar R, Schiavi SC.** FGF-23 inhibits renal tubular phosphate transport and is a PHEX substrate. *Biochem Biophys Res Commun* 284: 977–981, 2001.
7. **Ecarot B, Glorieux FH, Desbarats M, Travers R, Labelle L.** Defective bone formation by Hyp mouse bone cells transplanted into normal mice: evidence in favor of an intrinsic osteoblast defect. *J Bone Miner Res* 7: 215–220, 1992.
8. **Feng JQ, Ward LM, Liu S, Lu Y, Xie Y, Yuan B, Yu X, Rauch F, Davis SI, Zhang S, Rios H, Drezner MK, Quarles LD, Bonewald LF, White KE.** Loss of DMP1 causes rickets and osteomalacia and identifies a role for osteocytes in mineral metabolism. *Nat Genet* 38: 1310–1315, 2006.
9. **Imel EA, Hui SL, Econs MJ.** FGF23 concentrations vary with disease status in autosomal dominant hypophosphatemic rickets. *J Bone Miner Res* 22: 520–526, 2007.
10. **Kurosu H, Ogawa Y, Miyoshi M, Yamamoto M, Nandi A, Rosenblatt KP, Baum MG, Schiavi S, Hu MC, Moe OW, Kuro-o M.** Regulation of fibroblast growth factor-23 signaling by klotho. *J Biol Chem* 281: 6120–6123, 2006.
11. **Larsson T, Davis SI, Garringer HJ, Mooney SD, Draman MS, Cullen MJ, White KE.** Fibroblast growth factor-23 mutants causing familial tumoral calcinosis are differentially processed. *Endocrinology* 146: 3883–3891, 2005.
12. **Larsson T, Marsell R, Schipani E, Ohlsson C, Ljunggren O, Tenenhouse HS, Juppner H, Jonsson KB.** Transgenic mice expressing fibroblast growth factor 23 under the control of the α1(I) collagen promoter exhibit growth retardation, osteomalacia, and disturbed phosphate homeostasis. *Endocrinology* 145: 3087–3094, 2004.
13. **Liu S, Guo R, Simpson LG, Xiao ZS, Burnham CE, Quarles LD.** Regulation of fibroblastic growth factor 23 expression but not degradation by PHEX. *J Biol Chem* 278: 37419–37426, 2003.
14. **Liu S, Quarles LD.** How fibroblast growth factor 23 works. *J Am Soc Nephrol* 18: 1637–1647, 2007.
15. **Liu S, Zhou J, Tang W, Jiang X, Rowe DW, Quarles LD.** Pathogenic role of Fgf23 in Hyp mice. *Am J Physiol Endocrinol Metab* 291: E38–E49, 2006.
16. **Lorenz-Depiereux B, Bastepe M, Benet-Pages A, Amyere M, Wagenstaller J, Muller-Barth U, Badenhoop K, Kaiser SM, Rittmaster RS, Shlossberg AH, Olivares JL, Loris C, Ramos FJ, Glorieux F, Vikkula M, Juppner H, Strom TM.** DMP1 mutations in autosomal recessive hypophosphatemia implicate a bone matrix protein in the regulation of phosphate homeostasis. *Nat Genet* 38: 1248–1250, 2006.
17. **Masuyama R, Stockmans I, Torrekens S, Van Looveren R, Maes C, Carmeliet P, Bouillon R, Carmeliet G.** Vitamin D receptor in chondrocytes promotes osteoclastogenesis and regulates FGF23 production in osteoblasts. *J Clin Invest* 116: 3150–3159, 2006.
18. **Miao D, Bai X, Panda D, McKee M, Karaplis A, Goltzman D.** Osteomalacia in hyp mice is associated with abnormal phex expression and with altered bone matrix protein expression and deposition. *Endocrinology* 142: 926–939, 2001.
19. **Miao D, Bai X, Panda DK, Karaplis AC, Goltzman D, McKee MD.** Cartilage abnormalities are associated with abnormal Phex expression and with altered matrix protein and MMP-9 localization in Hyp mice. *Bone* 34: 638–647, 2004.
20. **Murshed M, Harmey D, Millan JL, McKee MD, Karsenty G.** Unique coexpression in osteoblasts of broadly expressed genes accounts for the spatial restriction of ECM mineralization to bone. *Genes Dev* 19: 1093–1104, 2005.
21. **Ogawa T, Onishi T, Hayashibara T, Sakashita S, Okawa R, Ooshima T.** Dentinal defects in Hyp mice not caused by hypophosphatemia alone. *Arch Oral Biol* 51: 58–63, 2006.
22. **Quarles LD, Drezner MK.** Effects of etidronate-mediated suppression of bone remodeling on aluminum-induced de novo bone formation. *Endocrinology* 131: 122–126, 1992.
23. **Reid IR, Murphy WA, Hardy DC, Teitelbaum SL, Bergfeld MA, Whyte MP.** X-linked hypophosphatemia: skeletal mass in adults assessed by histomorphometry, computed tomography, and absorptiometry. *Am J Med* 90: 63–69, 1991.
24. **Shimada T, Hasegawa H, Yamazaki Y, Muto T, Hino R, Takeuchi Y, Fujita T, Nakahara K, Fukumoto S, Yamashita T.** FGF-23 is a potent regulator of vitamin D metabolism and phosphate homeostasis. *J Bone Miner Res* 19: 429–435, 2004.
25. **Shimada T, Kakitani M, Yamazaki Y, Hasegawa H, Takeuchi Y, Fujita T, Fukumoto S, Tomizuka K, Yamashita T.** Targeted ablation of Fgf23 demonstrates an essential physiological role of FGF23 in phosphate and vitamin D metabolism. *J Clin Invest* 113: 561–568, 2004.
26. **Shimada T, Mizutani S, Muto T, Yoneya T, Hino R, Takeda S, Takeuchi Y, Fujita T, Fukumoto S, Yamashita T.** Cloning and characterization of FGF23 as a causative factor of tumor-induced osteomalacia. *Proc Natl Acad Sci USA* 98: 6500–6505, 2001.
27. **Shimada T, Muto T, Urakawa I, Yoneya T, Yamazaki Y, Okawa K, Takeuchi Y, Fujita T, Fukumoto S, Yamashita T.** Mutant FGF-23 responsible for autosomal dominant hypophosphatemic rickets is resistant to proteolytic cleavage and causes hypophosphatemia in vivo. *Endocrinology* 143: 3179–3182, 2002.
28. **Sitara D, Razzaque MS, Hesse M, Yoganathan S, Taguchi T, Erben RG, Juppner H, Lanske B.** Homozygous ablation of fibroblast growth factor-23 results in hyperphosphatemia and impaired skeletogenesis, and reverses hypophosphatemia in Phex-deficient mice. *Matrix Biol* 23: 421–432, 2004.
29. **Strom TM, Francis F, Lorenz B, Boddrich A, Econs MJ, Lehrach H, Meitinger T.** Pex gene deletions in Gy and Hyp mice provide mouse models for X-linked hypophosphatemia. *Hum Mol Genet* 6: 165–171, 1997.
30. **Tanaka H, Seino Y.** Direct action of 1,25-dihydroxyvitamin D on bone: VDRKO bone shows excessive bone formation in normal mineral condition. *J Steroid Biochem Mol Biol* 89–90: 343–345, 2004.
31. **The ADHR Consortium.** Autosomal dominant hypophosphataemic rickets is associated with mutations in FGF23. *Nat Genet* 26: 345–348, 2000.

32. **The HYP Consortium.** A gene (PEX) with homologies to endopeptidases is mutated in patients with X-linked hypophosphatemic rickets. *Nat Genet* 11: 130–136, 1995.
33. **Turner AJ, Tanzawa K.** Mammalian membrane metallopeptidases: NEP, ECE, KELL, and PEX. *FASEB J* 11: 355–364, 1997.
34. **Urakawa I, Yamazaki Y, Shimada T, Iijima K, Hasegawa H, Okawa K, Fujita T, Fukumoto S, Yamashita T.** Klotho converts canonical FGF receptor into a specific receptor for FGF23. *Nature* 444: 770–774, 2006.
35. **Weber TJ, Liu S, Indridason OS, Quarles LD.** Serum FGF23 levels in normal and disordered phosphorus homeostasis. *J Bone Miner Res* 18: 1227–1234, 2003.
36. **White KE, Carn G, Lorenz-Depiereux B, Benet-Pages A, Strom TM, Econs MJ.** Autosomal-dominant hypophosphatemic rickets (ADHR) mutations stabilize FGF-23. *Kidney Int* 60: 2079–2086, 2001.
37. **White KE, Jonsson KB, Carn G, Hampson G, Spector TD, Mannstadt M, Lorenz-Depiereux B, Miyauchi A, Yang IM, Ljunggren O, Meitinger T, Strom TM, Juppner H, Econs MJ.** The autosomal dominant hypophosphatemic rickets (ADHR) gene is a secreted polypeptide overexpressed by tumors that cause phosphate wasting. *J Clin Endocrinol Metab* 86: 497–500, 2001.
38. **Xiao ZS, Crenshaw M, Guo R, Nesbitt T, Drezner MK, Quarles LD.** Intrinsic mineralization defect in Hyp mouse osteoblasts. *Am J Physiol Endocrinol Metab* 275: E700–E708, 1998.
39. **Yamazaki Y, Okazaki R, Shibata M, Hasegawa Y, Satoh K, Tajima T, Takeuchi Y, Fujita T, Nakahara K, Yamashita T, Fukumoto S.** Increased circulatory level of biologically active full-length FGF-23 in patients with hypophosphatemic rickets/osteomalacia. *J Clin Endocrinol Metab* 87: 4957–4960, 2002.